Full wave inversion in Riemannian manifolds for zones with rugged topography

César A. Arias

Universidad de Antioquia, Instituto Tecnológico Metropolitano

April 11 2016

Introduction

The search of oil and gas are based on algorithms that generate tomographies of the earth's subsurface using seismic waves.
They are designed for domains with straight boundaries, but the oilfields are also found under rugged regions

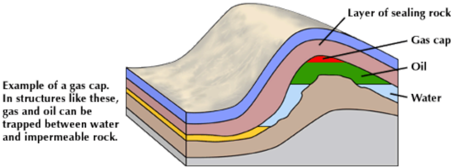

Figure: oil trap

Figure: Cusiana oilfield in Colombia

Figure: Oilfields in complex topography

Introduction

The procedure to generate images of the subsurface is to compare the real data collected by the geophones with the synthetic data generated by computational simulations: the solution of the wave equation. A cartesian mesh can not be well adapted to the geometry of the problem when the surface in not flat. Because of this, distorsions in the image are generated.

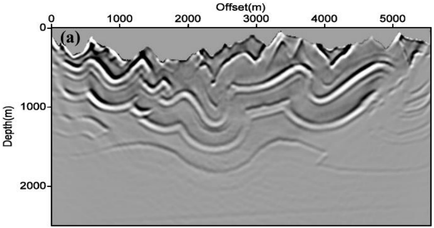

Figure: image formed with a cartesian mesh (C. Li y J.P. Huang,2014)

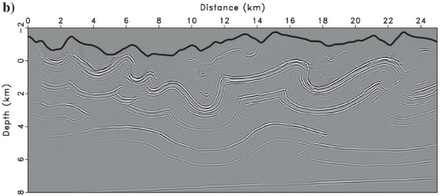

Figure: image formed from a generalized coordinate system (Shragge, J., 2014)

Introduction

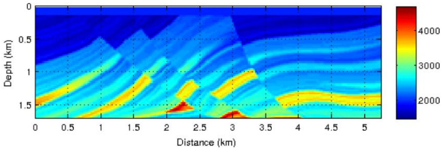

Figure: example of tomography with a flat upper boundary

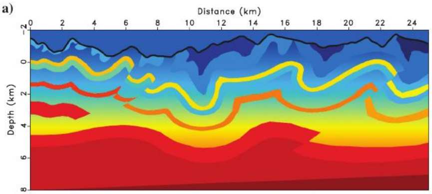

Figure: example of velocity model for complex topography

State of the art

The algorithms that generate the images are based on the comparison of the data received by the geophones (after the seismic waves are reflected in the different structures of the subsurface) with the simulated data.

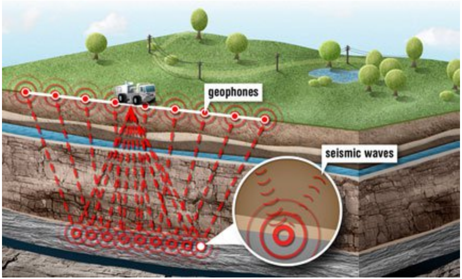

Figure: The construction of images of the earth's subsurface is based on the reflection of seismic waves

State of the art - Cartesian modeling

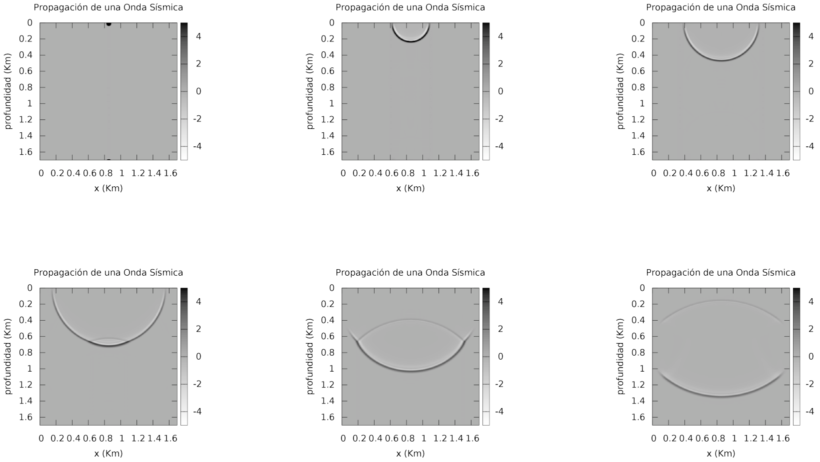

Figure: Seismic wavefronts in $t = 1, 100, 200, 300, 400y500$ milliseconds

State of the art - Cartesian modeling

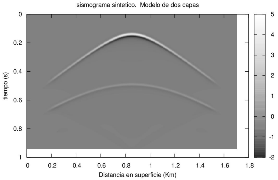

Figure: Synthetic seismogram for a model of 2 layers of constant propagation velocities

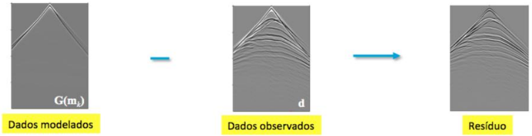

Figure: To search the right velocity model the difference of the synthetic en real seismograms is minimized

Theory of seismic tomography

$$E(\mathbf{m}) = \frac{1}{2}\Delta\mathbf{p}^{\dagger}\Delta\mathbf{p} = \frac{1}{2}\Delta\mathbf{p}^{T}\Delta\mathbf{p}^{*} = \frac{1}{2}\sum_{r=1}^{ng}\sum_{s=1}^{ns}\int_{0}^{t_{\max}} \mathrm{d}t|p_{cal}(\mathbf{x}_r, t; \mathbf{x}_s) - p_{obs}(\mathbf{x}_r, t; \mathbf{x}_s)|^2$$

A second-order Taylor-Lagrange development of the misfit function in the vicinity of $\mathbf{m}_0$ gives the expression

$$E(\mathbf{m}_0+\Delta\mathbf{m}) = E(\mathbf{m}_0)+\sum_{i=1}^{M}\frac{\partial E(\mathbf{m}_0)}{\partial m_i}\Delta m_i+\frac{1}{2}\sum_{i=1}^{M}\sum_{j=1}^{M}\frac{\partial^2 E(\mathbf{m}_0)}{\partial m_i \partial m_j}\Delta m_i \Delta m_j+O(||\Delta\mathbf{m}||^3)$$

Theory of seismic tomography

Taking the derivative with respect to the model parameter m_i results in

$$\frac{\partial E(\mathbf{m})}{\partial m_i} = \frac{\partial E(\mathbf{m}_0)}{\partial m_i} + \sum_{j=1}^{M} \frac{\partial^2 E(\mathbf{m}_0)}{\partial m_j \partial m_i} \Delta m_j, i = 1, 2, \ldots, M.$$

Briefly speaking, it is

$$\frac{\partial E(\mathbf{m})}{\partial \mathbf{m}} = \frac{\partial E(\mathbf{m}_0)}{\partial \mathbf{m}} + \frac{\partial^2 E(\mathbf{m}_0)}{\partial \mathbf{m}^2} \Delta \mathbf{m}$$

Thus,

$$\Delta \mathbf{m} = -\left(\frac{\partial^2 E(\mathbf{m}_0)}{\partial \mathbf{m}^2}\right)^{-1} \frac{\partial E(\mathbf{m}_0)}{\partial \mathbf{m}} = -\mathbf{H}^{-1} \nabla E_{\mathbf{m}}$$

Theory of seismic tomography

where

$$\nabla E_{\mathbf{m}} = \frac{\partial E(\mathbf{m}_0)}{\partial \mathbf{m}} = \left[\frac{\partial E(\mathbf{m}_0)}{\partial m_1}, \frac{\partial E(\mathbf{m}_0)}{\partial m_2}, \ldots, \frac{\partial E(\mathbf{m}_0)}{\partial m_M}\right]^T$$

and

$$\mathbf{H} = \frac{\partial^2 E(\mathbf{m}_0)}{\partial \mathbf{m}^2} = \left[\frac{\partial^2 E(\mathbf{m}_0)}{\partial m_i \partial m_j}\right] = \begin{bmatrix} \frac{\partial^2 E(\mathbf{m}_0)}{\partial m_1^2} & \frac{\partial^2 E(\mathbf{m}_0)}{\partial m_1 m_2} & \cdots & \frac{\partial^2 E(\mathbf{m}_0)}{\partial m_1 m_M} \\ \frac{\partial^2 E(\mathbf{m}_0)}{\partial m_2 m_1} & \frac{\partial^2 E(\mathbf{m}_0)}{\partial m_2^2} & \cdots & \frac{\partial^2 E(\mathbf{m}_0)}{\partial m_2 m_M} \\ \vdots & & \ddots & \vdots \\ \frac{\partial^2 E(\mathbf{m}_0)}{\partial m_M m_1} & \frac{\partial^2 E(\mathbf{m}_0)}{\partial m_M m_2} & \cdots & \frac{\partial^2 E(\mathbf{m}_0)}{\partial m_M^2} \end{bmatrix}.$$

$\nabla E_{\mathbf{m}}$ and $\mathbf{H}$ are the gradient vector and the Hessian matrix, respectively.

Theory of seismic tomography

$$
\begin{aligned}
\frac{\partial E(\mathbf{m})}{\partial m_i} &= \frac{1}{2}\sum_{r=1}^{ng}\sum_{s=1}^{ns}\int \mathrm{d}t \left[\left(\frac{\partial p_{cal}}{\partial m_i}\right)(p_{cal}-p_{obs})^* + \left(\frac{\partial p_{cal}}{\partial m_i}\right)^*(p_{cal}-p_{obs})\right] \\
&= \sum_{r=1}^{ng}\sum_{s=1}^{ns}\int \mathrm{d}t\,\mathtt{Re}\left[\left(\frac{\partial p_{cal}}{\partial m_i}\right)^*\Delta p\right] (\Delta p = p_{cal}-p_{obs}) \\
&= \mathtt{Re}\left[\left(\frac{\partial \mathbf{p}_{cal}}{\partial m_i}\right)^\dagger \Delta\mathbf{p}\right] = \mathtt{Re}\left[\left(\frac{\partial \mathbf{f}(\mathbf{m})}{\partial m_i}\right)^\dagger \Delta\mathbf{p}\right], i = 1, 2, \ldots, M.
\end{aligned}
$$

That is to say,

$$
\nabla E_{\mathbf{m}} = \nabla E(\mathbf{m}) = \frac{\partial E(\mathbf{m})}{\partial \mathbf{m}} = \mathtt{Re}\left[\left(\frac{\partial \mathbf{f}(\mathbf{m})}{\partial \mathbf{m}}\right)^\dagger \Delta\mathbf{p}\right] = \mathtt{Re}\left[\mathbf{J}^\dagger \Delta\mathbf{p}\right]
$$

where Re takes the real part, and $\mathbf{J} = \frac{\partial \mathbf{p}_{cal}}{\partial \mathbf{m}} = \frac{\partial \mathbf{f}(\mathbf{m})}{\partial \mathbf{m}}$ is the Jacobian matrix, i.e. sensitivity or the Fréchet derivative matrix.

Theory of seismic tomography

Recall that the basic acoustic wave equation can be specified as

$$\frac{1}{v^2(\mathbf{x})}\frac{\partial^2 p(\mathbf{x},t;\mathbf{x}_s)}{\partial t^2} - \nabla^2 p(\mathbf{x},t;\mathbf{x}_s) = f_s(\mathbf{x},t;\mathbf{x}_s).$$

where $f_s(\mathbf{x},t;\mathbf{x}_s) = f(t')\delta(\mathbf{x}-\mathbf{x}_s)\delta(t-t')$. The Green's function $\Gamma(\mathbf{x},t;\mathbf{x}_s,t')$ is defined by

Theory of seismic tomography

Thus the integral representation of the solution can be given by

$$
\begin{aligned}
p(\mathbf{x}_r, t; \mathbf{x}_s) &= \int_V \mathrm{d}\mathbf{x} \int \mathrm{d}t' \Gamma(\mathbf{x}_r, t; \mathbf{x}, t') f(\mathbf{x}, t'; \mathbf{x}_s) \\
&= \int_V \mathrm{d}\mathbf{x} \int \mathrm{d}t' \Gamma(\mathbf{x}_r, t - t'; \mathbf{x}, 0) f(\mathbf{x}, t'; \mathbf{x}_s) (\text{Causility of Green's function}) \\
&= \int_V \mathrm{d}\mathbf{x} \Gamma(\mathbf{x}_r, t; \mathbf{x}, 0) * f(\mathbf{x}, t; \mathbf{x}_s)
\end{aligned}
$$

Theory of seismic tomography

A perturbation $v(\mathbf{x}) \to v(\mathbf{x}) + \Delta v(\mathbf{x})$ will produce a field $p(\mathbf{x}, t; \mathbf{x}_s) + \Delta p(\mathbf{x}, t; \mathbf{x}_s)$ defined by

$$\frac{1}{(v(\mathbf{x}) + \Delta v(\mathbf{x}))^2} \frac{\partial^2 [p(\mathbf{x}, t; \mathbf{x}_s) + \Delta p(\mathbf{x}, t; \mathbf{x}_s)]}{\partial t^2} - \nabla^2 [p(\mathbf{x}, t; \mathbf{x}_s) + \Delta p(\mathbf{x}, t; \mathbf{x}_s)] = f_s(\mathbf{x}, t; \mathbf{x}_s)$$

Note that

$$\frac{1}{(v(\mathbf{x}) + \Delta v(\mathbf{x}))^2} = \frac{1}{v^2(\mathbf{x})} - \frac{2\Delta v(\mathbf{x})}{v^3(\mathbf{x})} + O(\Delta^2 v(\mathbf{x}))$$

Theory of seismic tomography

$$\frac{1}{v^2(\mathbf{x})}\frac{\partial^2 \Delta p(\mathbf{x},t;\mathbf{x}_s)}{\partial t^2} - \nabla^2 \Delta p(\mathbf{x},t;\mathbf{x}_s) = \frac{\partial^2 [p(\mathbf{x},t;\mathbf{x}_s) + \Delta p(\mathbf{x},t;\mathbf{x}_s)]}{\partial t^2}\frac{2\Delta v(\mathbf{x})}{v^3(\mathbf{x})}$$

$$\frac{1}{v^2(\mathbf{x})}\frac{\partial^2 \Delta p(\mathbf{x},t;\mathbf{x}_s)}{\partial t^2} - \nabla^2 \Delta p(\mathbf{x},t;\mathbf{x}_s) = \frac{\partial^2 p(\mathbf{x},t;\mathbf{x}_s)}{\partial t^2}\frac{2\Delta v(\mathbf{x})}{v^3(\mathbf{x})}$$

Again, based on integral representation, we obtain

$$\Delta p(\mathbf{x}_r,t;\mathbf{x}_s) = \int_V \mathrm{d}\mathbf{x}\Gamma(\mathbf{x}_r,t;\mathbf{x},0) * \frac{\partial^2 p(\mathbf{x},t;\mathbf{x}_s)}{\partial t^2}\frac{2\Delta v(\mathbf{x})}{v^3(\mathbf{x})}.$$

Theory of seismic tomography

According to the previous section, it follows that

$$\frac{\partial p_{cal}}{\partial v_i(\mathbf{x})} = \int_V \mathrm{d}\mathbf{x}\Gamma(\mathbf{x}_r, t; \mathbf{x}, 0) * \ddot{p}(\mathbf{x}, t; \mathbf{x}_s)\frac{2}{v^3(\mathbf{x})} = \int_V \mathrm{d}\mathbf{x}\Gamma(\mathbf{x}_r, t; \mathbf{x}, 0) * \frac{\partial^2 p(\mathbf{x}, t; \mathbf{x}_s)}{\partial t^2}\frac{2}{v^3(\mathbf{x})}.$$

The convolution guarantees

$$\int \mathrm{d}t[g(t) * f(t)]h(t) = \int \mathrm{d}t f(t)[g(-t) * h(t)].$$

Theory of seismic tomography

$$
\begin{aligned}
\frac{\partial E(\mathbf{m})}{\partial m_i} &= \sum_{r=1}^{ng}\sum_{s=1}^{ns}\int \mathrm{d}t\mathrm{Re}\left[\left(\frac{\partial p_{cal}}{\partial m_i}\right)^{*}\Delta p\right] \; (\Delta p = p_{cal} - p_{obs}) \\
&= \sum_{r=1}^{ng}\sum_{s=1}^{ns}\int_0^{t_{\max}} \mathrm{d}t\mathrm{Re}\left[\left(\int_V \mathrm{d}\mathbf{x}\Gamma(\mathbf{x}_r, t; \mathbf{x}, 0) * \frac{\partial^2 p(\mathbf{x}, t; \mathbf{x}_s)}{\partial t^2}\frac{2}{v^3(\mathbf{x})}\right)^{*}\Delta p(\mathbf{x}_r, t; \mathbf{x}_s)\right] \\
&= \sum_{r=1}^{ng}\sum_{s=1}^{ns}\int_0^{t_{\max}} \mathrm{d}t\mathrm{Re}\left[\left(\frac{\partial^2 p_{cal}(\mathbf{x}, t; \mathbf{x}_s)}{\partial t^2}\frac{2}{v^3(\mathbf{x})}\right)^{*}\left(\int_V \mathrm{d}\mathbf{x}\Gamma(\mathbf{x}_r, -t; \mathbf{x}, 0) * \Delta p(\mathbf{x}_r, t; \mathbf{x}_s)\right)\right] \\
&= \sum_{r=1}^{ng}\sum_{s=1}^{ns}\int_0^{t_{\max}} \mathrm{d}t\mathrm{Re}\left[\left(\frac{\partial^2 p_{cal}(\mathbf{x}, t; \mathbf{x}_s)}{\partial t^2}\frac{2}{v^3(\mathbf{x})}\right)^{*}\left(\int_V \mathrm{d}\mathbf{x}\Gamma(\mathbf{x}_r, 0; \mathbf{x}, t) * \Delta p(\mathbf{x}_r, t; \mathbf{x}_s)\right)\right] \\
&= \sum_{r=1}^{ng}\sum_{s=1}^{ns}\int_0^{t_{\max}} \mathrm{d}t\mathrm{Re}\left[\left(\frac{\partial^2 p_{cal}(\mathbf{x}, t; \mathbf{x}_s)}{\partial t^2}\frac{2}{v^3(\mathbf{x})}\right)^{*} p_{res}(\mathbf{x}_r, t; \mathbf{x}_s)\right]
\end{aligned}
$$

Theory of seismic tomography

where $p_{res}(\mathbf{x}, t; \mathbf{x}_s)$ is a time-reversal wavefield produced using the residual $\Delta p(\mathbf{x}_r, t; \mathbf{x}_s)$ as the source. It follows from reciprocity theorem

$$p_{res}(\mathbf{x}, t; \mathbf{x}_s) = \int_V \mathrm{d}\mathbf{x}\Gamma(\mathbf{x}_r, 0; \mathbf{x}, t) * \Delta p(\mathbf{x}_r, t; \mathbf{x}_s) = \int_V \mathrm{d}\mathbf{x}\Gamma(\mathbf{x}, 0; \mathbf{x}_r, t) * \Delta p(\mathbf{x}_r, t; \mathbf{x}_s).$$

satisfying

$$\frac{1}{v^2(\mathbf{x})}\frac{\partial^2 p_{res}(\mathbf{x}, t; \mathbf{x}_s)}{\partial t^2} - \nabla^2 p_{res}(\mathbf{x}, t; \mathbf{x}_s) = \Delta p(\mathbf{x}_r, t; \mathbf{x}_s).$$

Seismic modeling in complex topography

The problem of the propagation of a seismic wave in complex topography can be transformed into the problem of propagation in a rectangular mesh by means of a coordinate transformation

$$\begin{bmatrix} x1 \\ x2 \end{bmatrix} = \begin{bmatrix} \xi_1 \\ \\ \xi_2 + \tau(\xi_1) \end{bmatrix} \tag{1}$$

where x_1 and x are the coordinates in the physical domain whose upper boundary is complex (not flat) and ξ_1 and ξ_2 are the coordinates of the rectangular domain. The function $\tau(x_1) = \tau(\xi_1)$ represents the upper edge of the physical domain, that is, the shape of the mountain.

Seismic modeling in complex topography

This transformation allows to map the rectangle to practically any topography. A uniform mesh in generated in the rectangle. The mesh lines are mapped into the physical domain, generating in this way the curved lines conformal to the topography

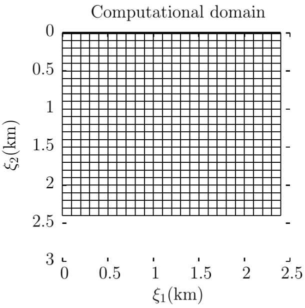

Figure: Uniform grid used for the computational domain

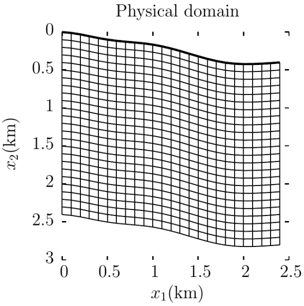

Figure: curved grid used for the physical domain

Wave equation in generalized coordinates

The rectangular mesh is discretized in the usual way. In the new coordinate system that is denoted ξ_1 and ξ_2 the wave equation is

$$\left[\nabla^2 - \frac{1}{v^2}\frac{\partial^2}{\partial t^2}\right] u(\xi_1, \xi_2) = f(\xi_1, \xi_2) \tag{2}$$

with

$$\nabla^2 = \frac{1}{\sqrt{|\boldsymbol{g}|}}\frac{\partial}{\partial \xi_i}\left(g^{ij}\sqrt{|\boldsymbol{g}|}\frac{\partial}{\partial \xi_j}\right) \qquad i, j = 1, 2, 3 \tag{3}$$

where

$$g_{ij} = \frac{\partial x_k}{\partial \xi_i}\frac{\partial x_k}{\partial \xi_j} \tag{4}$$

are the metric coefficients and $|\boldsymbol{g}|$ is the absolute value of the determinant.

Example: 2 layers model

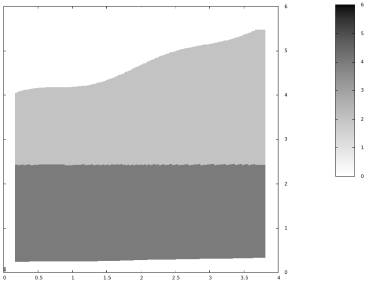

Figure: 2 velocities model

Seismic modeling in complex topography

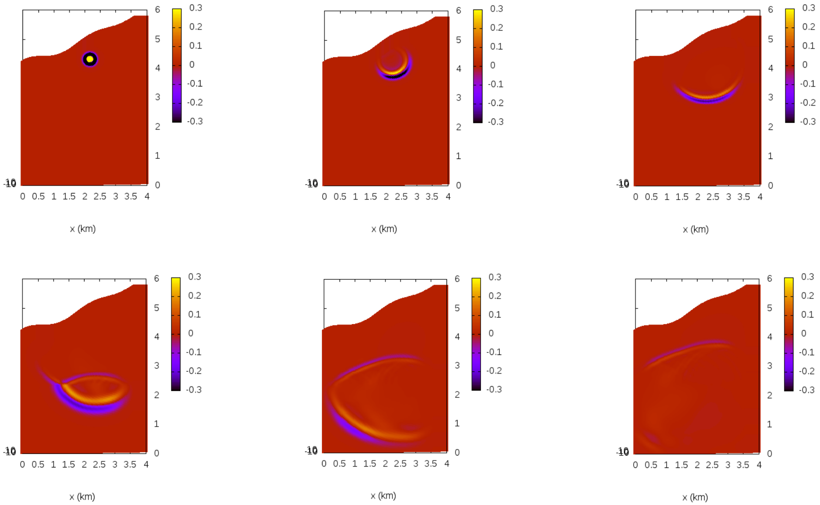

Figure: Seismic wavefront

Seismic modeling in complex topography

In the rectangular domain seismograms can be generated just by taking a sample of the field in $\xi = cte$, tha corresponds to a sample of the field over the upper edge of the physical domain.

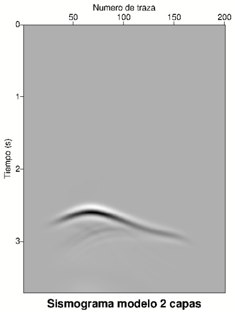

Figure: seismogram obtained in $\xi = 4$ in the rectangular domain

Results for tomography in a curved mesh

The FWI algorithm was applied to the Canadian Foothills SEG velocity model. A synthetic model for a zone in British Columbia (Canada) that presents several common geological features of that region.

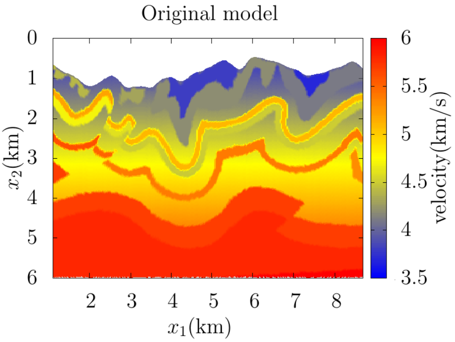

Figure: Canadian Foothills SEG velocity model

Results for tomography in a curved mesh

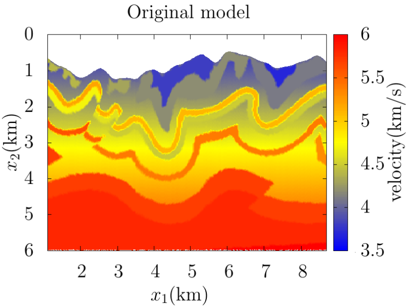

Figure: Original Canadian Foothills SEG model

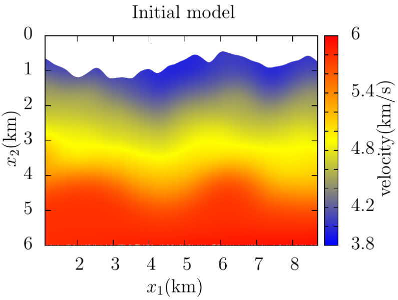

Figure: Model used to start the FWI algrithm

Results for tomography in a curved mesh

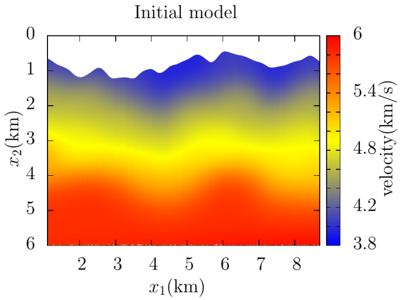

Figure: Model used to start the FWI algrithm

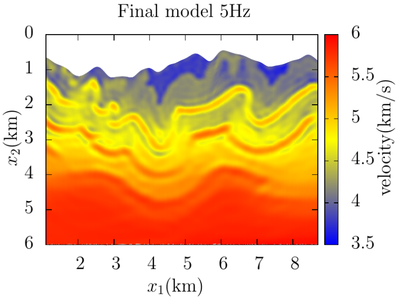

Figure: Final velocity after 200 iterations using a 5hz source

Results for tomography in a curved mesh

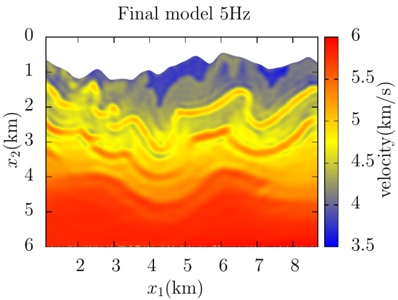

Figure: Final model after 200 iterations using a 5hz source

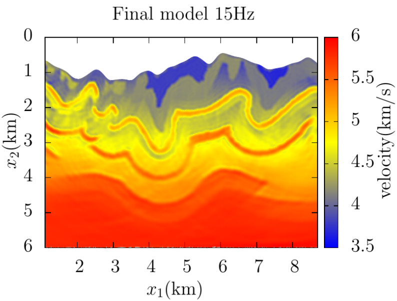

Figure: Final velocity after 200 iterations using a 15hz source

Results for tomography in a curved mesh

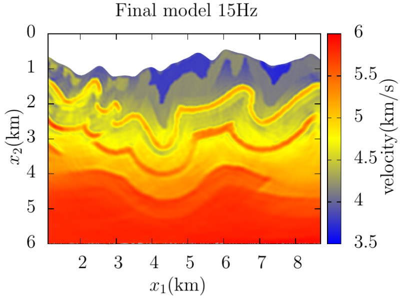

Figure: Final velocity after 200 iterations using a 15hz source

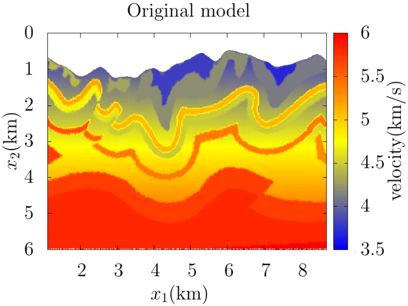

Figure: Original velocity model

Convergence

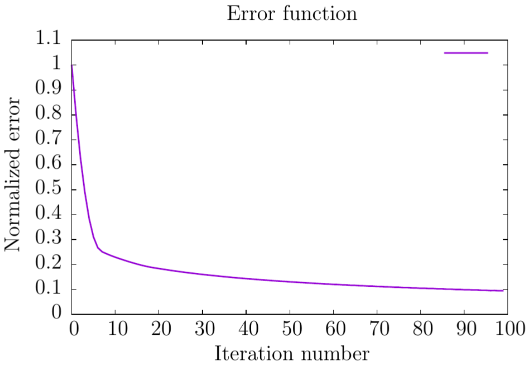

Figure: Convergence of the FWI algorithm in Riemannian space

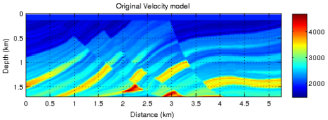

(a) Original velocity model "**v**".

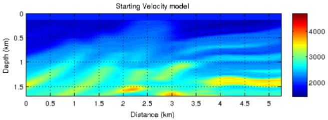

(b) Starting velocity model "$\mathbf{v_0}$"

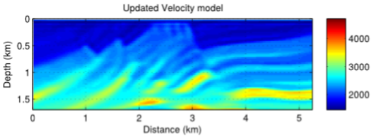

(c) Updated velocity model "$\mathbf{v_f}$".

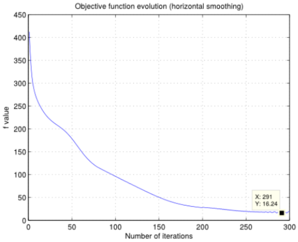

(d) Objective function's evol.

Figure: FWI in an Euclidian space for the Marmousi velocity model

Usual FWI

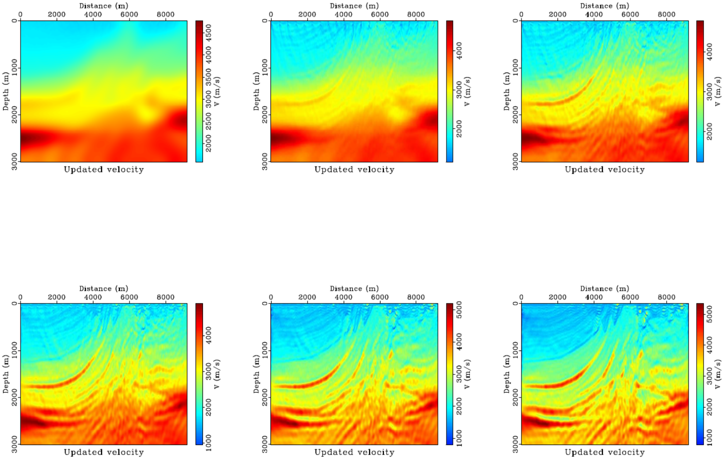

Figure 17: The updated velocity model at the iteration 1, 20, 50, 100, 180 and 300.

Figure: FWI in an Euclidian space for the Marmousi velocity model

Conclusions

- FWI can be implemented in curved meshes just by modifying the laplacian.
- When transforming from physical to computational domain the steps sizes in time and space doesn't change.
- The algorithms also solves the problem of the near-surface imaging.
- The transformantion can be applied to other wave equations using the chaing rule for the derivatives.

Bibliography

- Berryhill, J., 1979, Wave-equation datuming, Geophysics , 44, No. 8, 1329-1344 http://dx.doi.org/10.1190/1.1441010
- Han, Y., Huang, J., Li, Z., Jia, L., 2015, Acoustic full waveform inversion method research in areas with rugged surface: Presented at the 2015 Annual International Meeting,SEG.http://dx.doi.org/10.1190/segam2015-5880195.1
- Liu, F., Guasch, L., Morton, S.A, Warner, M., Umpleby, A., Meng, Z., Fairhead, S. and Checkles, S., 2012, 3-D Time- domain full waveform inversion of a Valhal OBC dataset: Presented at the 2012 Annual International Meeting, SEG. http://dx.doi.org/10.1190/segam2012-1105.1
- Plessix, R.-E, 2006, A review of the adjoint-state method for computing the gradient of a functional with geophysical applications, Geophysics Journal International, 167, No. 2, 495-503. http://dx.doi.org/10.1111/j.1365-246X.2006.02978.x
- Shragge, J., 2014, Solving the 3D acoustic wave equation on generalized structured meshes: A finite-difference time- domain approach: Geophysics, 79, No. 6, 1-16. http://dx.doi.org/10.1190/geo2014-0172.1

Bibliography

- Shragge, J., 2014, Reverse time migration from topography, Geophysics, 79, No. 4, 1-12. http://dx.doi.org/10.1190/geo2013-0405.1
- Synge, J. L., and A. Schild, 1978, Tensor calculus: Dover Publications. namely the quadratic error function
- Tarantola, A., 1984, Inversion of seismic reflection data in the acoustic approximation: Geophysics, 49, No. 8, 1259- 1266. http://dx.doi.org/10.1190/1.1441754
- Virieux, J., and S. Operto, 2009, An overview of full waveform inversion in exploration geophysics: Geophysics,74, No. 6, WCC1–WCC26. http://dx.doi.org/10.1190/1.3238367